Heliyon 10 (2024) e32837

Contents lists available at ScienceDirect

Heliyon

journal homepage: www.cell.com/heliyon

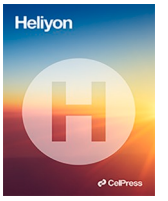

Research article

The effect of fish collagen on the silver nanoparticles sizes and shapes using modified microwave-assisted green synthesis method and their antibacterial activities

Mustafa Mudhafar [a,b,**], Ismail Zainol [c,*], Ameer A.J. [d], Mena Y. Abd [e], H.A. Alsailawi [e,f], Nouby M. Ghazaly [g,h], Rafal Muhammed Hussein [i], Mohammed Zorah [j]

[a] Department of Medical Physics, Faculty of Medical Applied Sciences, University of Kerbala, 56001, Karbala, Iraq
[b] Department of Anesthesia Techniques and Intensive Care, Al-Taff university college, 56001, Kerbala, Iraq
[c] Department of Chemistry, Faculty of Science and Mathematics, Universiti Pendidikan Sultan Idris, 35900 Tanjung Malim, Perak, Malaysia
[d] Al-Zahraa University for Women, Karbala, Iraq
[e] Department of biochemistry, Faculty of Medicine, University of Kerbala, 56001, Karbala, Iraq
[f] Department of Anesthesia Techniques, AlSafwa University College, Karbala, Iraq
[g] Technical College, Imam Ja'afar Al-Sadiq University, Baghdad, Iraq
[h] Mechanical Engineering, Faculty of Engineering, South Valley University, Egypt
[i] Karbala veterinary Hospital, Iraq
[j] Department of C. T. E, Imam Al-Kadhum College, Baghdad, Iraq

ARTICLE INFO

Keywords:
Microwave-assisted green synthesis
Melia dubia leaves
Fish collagen
Silver nano particles

ABSTRACT

This work aimed to produce silver nanoparticles (AgNPs) by efficient green synthesis techniques, namely rapid green synthesis and modified microwave-assisted green synthesis methods. The study used fish scale collagen (FsCol) as a stabilizer to assess its impact on the dimensions and configurations of AgNPs. Four samples were prepared with varying concentrations of FsCol. The synthesized AgNPs were characterized using Ultraviolet–visible (UV–vis) spectroscopy, scanning electron microscope (SEM), energy dispersive X-ray analysis (EDX), Fourier Transform Infrared Spectroscopy (FTIR), X-Ray diffraction analysis (XRD), Dynamic Light Scattering (DLS), and Transmission electron microscopy (TEM) techniques. The obtained sizes are as follows: 85 ± 15 nm, 70 ± 10 nm, 50 ± 10 nm, and 28–40 nm. The UV–vis spectroscopy revealed a shift in the absorbance peaks from 400 to 446 nm. The SEM method showed a spherical form in all of the samples. The element silver was detected in the EDX examination, along with the presence of oxygen (O) and carbon (C). The FTIR analysis revealed that the peaks seen at 3307 cm^{-1} were attributed to the stretching of O–H bonds, while the mountain at 1638 cm^{-1} belonged to the extension of N–H bonds (amide A). Additionally, the band observed at 1638 cm^{-1} indicated the presence of CO bonds (amide I).The 2140 cm^{-1} and 1302 cm^{-1} peaks may be attributed to the C_2H_2 group present in the plant components and the N–H bending (Amide III), respectively. The XRD pattern indicates that the synthesis process resulted in the formation of crystalline AgNPs. The particle sizes measured using DLS were 121 nm, 96.36 nm, 82.3 nm, and 48.50 nm. The TEM approach revealed that all samples had a spherical morphology with varying sizes: 80–100 nm,

* Corresponding author.
** Corresponding author.
E-mail addresses: almosawy2014@gmail.com (M. Mudhafar), ismail.zainol@fsmt.upsi.edu.my (I. Zainol).

https://doi.org/10.1016/j.heliyon.2024.e32837
Received 1 December 2023; Received in revised form 2 May 2024; Accepted 10 June 2024
Available online 11 June 2024

50–80 nm, 40–60 nm, and 28–42 nm. The synthesized AgNPs were tested for their antibacterial properties against the pathogenic pathogens *Escherichia coli* (*E.coli)* and *Staphylococcus aureus (S. aureus)*. The influence of AgNPs on bacteria was amplified as the particle size decreased, resulting in a larger inhibitory zone for the smaller particles.

1. Introduction

AgNPs are often used in various applications, such as cleaning agents, business spaces, food storage, healthcare goods, packaging, and textile coating. These compounds possess antibacterial qualities that make them suitable for environmental applications since they can effectively attack bacteria, fungi, and viruses. Biomedical products such as topical lotions, antibacterial sprays, and wound dressings are often used. This occurs because they can impede the enzymatic functions of microbes by disrupting the membranes of these detrimental organisms [1,2].

AgNPs may be synthesized using three primary methods: chemical, physical, and biological processes. Lately, the primary focus of researchers has been on the techniques devised for producing AgNPs using green chemistry. The variables of decrease, narrowing, and steadiness determine it. This approach used environmentally benign and harmless biological substances to create AgNPs. Utilizing natural extracts derived from biological materials or creatures, such as enzymes, vitamins, amino acids, and polysaccharides, is a method that is ecologically sustainable but entails significant chemical intricacy.

Using plant extracts to synthesize AgNPs is advantageous owing to its accessibility, lack of toxicity, and safety. The sections often include diverse metabolites that may efficiently reducing silver ions, usually quicker than microbial production. The presence of phytochemicals makes plant-assisted reduction the primary mechanism for the process. The phytochemicals are aldehydes, amides, carboxylic acids, flavones, and ketones. The process responsible for quickly removing ions is attributed to flavones, organic acids, quinones, and phytochemicals that may dissolve in water [3]. Multiple studies have shown that xerophytes have contributed to creating AgNPs. Xerophytes possess emodin, an anthraquinone that undergoes tautomerization. Concurrently, it was found that mesophytes had three specific benzoquinones: hydroquinone, dietchequinone, and stay. Phytochemicals are often used for ion reduction and the production of AgNPs [4]. Although the biological processing techniques had some qualities, they were shown to be less efficient compared to the chemical approaches. The chemical procedures were combined with the natural approaches to counteract this adverse effect. Microwave irradiation induces rapid and even heating, facilitating homogeneous nucleation and growth.

Melia dubia, sometimes called neem, belongs to the *Melia* genus in the *Meliaceae* family. It is prevalent in India and Malaysia. The nanosilver with potential anticancer action has been synthesized using the Indian *Melia dubia* extract using $AgNO_3$. Kathiravan et al. [5] have produced AgNPs with anticancer properties.According to previous studies, a wide range of stabilizers was used to cap the AgNPs, such as gelatin [6], polyvinylpyrrolidone (PVP) [7], and poly(vinyl alcohol) [8]. Many of these studies used a chemical stabilizer that may cause toxicity for the final product. In the present study, a natural stabilizer, was collagen from the scales of fish (natural source), was used as a stabilizer agent.

A few studies in the literature were reported to examine the impact of stabilizers on the nanosilver particles' size, such as PVA [9]. This study is the first report to study the effect of FsCol as a stabilizer concentration has been studied. Various concentrations of FsCol were used to achieve four distinct sizes. The synthesized AgNPs were categorised using UV–vis spectroscopy, FESEM, XRD, FTIR, DLS, and Teethe antibacterial efficacy of the synthesized silver nanoparticle was assessed against several bacterial strains, yielding favourable outcomes against all of them. This conclusion validates the products gained from the previous investigation, wherein the production of nanometals has substantial antibacterial properties.

2. Description of materials and procedures

2.1. Materials used

The $AgNO_3$ was purchased from Bendosen, whereas the *M. dubia* leaves were locally sourced from Perak, Malaysia. The collagen was extracted from the fish scales at the Chemistry Department laboratory at UPSI, Perak, Malaysia. The broth and nutrient agar were purchased from Merck.

2.2. Preparation of M. dubia leaves

Perak was the source of freshly gathered *M. dubia* leaves. The leaves underwent many purification processes to eradicate dust and fungus, followed by a week-long sun-drying period to eliminate moisture. The desiccated foliage was transformed into a fine powder using pulverization. Ten grams of dry powder were extracted using 100 ml of distilled water in a 250 ml conical flask. Subsequently, the powder was subjected to a 10-min heating process, followed by cooling and filtration to get a raw extract. The extract was then incubated at a temperature of 4 °C.

2.3. Modified microwave-assisted green synthesis of AgNPs

AgNPs of different sizes were synthesized using the microwave-assisted green method. A 1×10^{-3} M solution of $AgNO_3$ was made

by dissolving it in 90 ml of distilled water in a 250 ml conical flask. A volume of 10 ml of crude extract was introduced into the solution to serve as a reducing agent. In addition, several quantities of fish collagen (0.1, 0.2, 0.4, and 0.6 g) were mixed with the solution to enhance its stability. The solutions were labeled as AgNPs-2, AgNPs-3, AgNPs-4, and AgNPs-5. The solution was inserted into the 800-W microwave oven and heated for 3 min. Upon examination, it was seen that the solution experienced a chromatic metamorphosis, transitioning from a state of colourlessness to a hue of yellow-brown. They analyzed the production of silver nanoparticles by UV–visible spectroscopy. The silver nanoparticle solution was centrifuged for 10 min at a rotational speed of 14000 revolutions per minute (rpm). The supernatant was discarded, while the nanoparticle fraction was sterilized using distilled water. The method above was iterated thrice to eradicate undesirable biomaterials and impurities [3]. A solitary specimen was meticulously created using an identical methodology to juxtapose the ramifications of microwave-assisted and non-microwave techniques. For the preparation, 0.1 g of collagen and an equivalent amount of silver nitrate, referred to as AgNPs-1, were used.

2.4. AgNPs analysis

The synthesized samples were analyzed using various analytical techniques, including EDX (Energy-dispersive X-ray spectroscopy), SEM (scanning electron microscope), UV–vis (UV–Visible Spectroscopy), FTIR (Fourier-transform infrared spectroscopy), X-RD (X-ray Powder Diffraction), DLS (dynamic light scattering), and TEM (transmission electron microscopy).

2.4.1. UV–vis spectroscopy

The concentration of an analyte in the solution can be determined by measuring the absorbance at a specific wavelength and applying the Beer-Lambert Law. 5 samples were prepared and kept for 24 h and measured the absorbance was between 200 and 800 nm.

2.4.2. SEM and EDX (FESEM)

EDX with SEM were used for the five prepared samples to elemental analysis of the particles which can provide a rapid qualitative and quantitative analysis of the elemental composition.

2.4.3. XRD

The interaction of the incident rays with the sample produces constructive interference (and a diffracted ray) when conditions satisfy Bragg's Law ($n\lambda = 2d\sin\theta$). This law relates the wavelength (λ) of electromagnetic radiation to the diffraction angle (θ) and the lattice spacing (d) in a crystalline sample. 5 samples were checked for XRD to know the particle size of each sample.

2.4.4. DLS

The DLS system has the ability to perform Autotitration measurements and Trend measurements, including the determination of the Protein melting point. All samples were checked by DLS to conform the size of Nano-particles.

2.4.5. TEM

To understand the morphology of AgNPs, transmission electron microscopy was used. TEM technique confirms the 2-dimensional structure of Nano and helps in measuring the lateral dimensions of Nano structures. To obtain the images for Nano-sheets samples before and after cation exchange, a drop of Nano-sheets sample diluted in toluene was drop 13 casted on a copper TEM grid and allowed to dry for several minutes. For TEM measurement, a beam of electrons is used to obtain the image of Nano.

2.4.6. FTIR

A small drop of silver nanoparticles was placed on the KBr plates. The second plate was put on top and made a quarter turn to obtain a nice even film. The plates were placed into the sample holder and run a spectrum. AgNPs have separated the plates and wipe one side clean before putting them back together. Thermo Scientific PerkinElmer Model: Spectrum 100 Spectrometers used to measure the FTIR spectra. KBr used as reference material and samples measured in the liquid form. From the range of 4400 to 300 cm^{-1} by averaging 200 scans at 2 cm^{-1} resolution, the spectra noted.

2.5. Bactericidal efficacy

The antibacterial studies utilized disc diffusion to evaluate the efficacy against Gram-negative *E.coli* and Gram-positive bacteria *S. aureus*. Bacteria were cultured using a nutrient agar media. The studied bacterial strains were inoculated from the stock cultures onto nutritional agar (NA) plates and then incubated for 24 h. Subsequently, the isolated bacterial colonies were used as inoculums. The bacteria were transferred to the autoclaved nutrient agar using a bacteriological loop. The solution was then cooled to a temperature of 450 °C using a water bath while gently agitating the flasks. The medium was then poured over the Petri plates to sterilize them and allow them to solidify for use in the biotest [4]. A new batch of inoculums from each culture was evenly spread over a nutrient agar medium in a Petri plate. Twenty microliter aliquots bearing a concentration of 5 μg per milliliter of as-synthesized silver nanoparticles were applied using a micropipette onto paper discs with a diameter of 6 mm. Five samples were produced for the bacterial test and labeled 1, 2, 3, 4, and 5, corresponding to AgNPs-1, AgNPs-2, AgNPs-3, AgNPs-4, and AgNPs-5, respectively. Subsequently, the silver nanoparticle solution samples were diluted in distilled water to achieve a concentration of 5 μ/mL. The measurement of inhibition zones was conducted after a 24-h incubation period.The antibacterial efficacy against gram-negative *Escherichia coli* and gram-positive

bacteria *Staphylococcus aureus* was assessed by measuring the size of the inhibition zones in the disc diffusion test. The exact process was replicated for the plant extract and ampicillin to determine their efficacy.

3. Results and discussion

At first, the silver nitrate solution had no color. After adding an extract of M.dubia and FsCol to the resolution, the color transitioned from colorless to yellow. This signifies the start of the formation of silver nanoparticles (AgNPs). The transition of the silver nitrate solution from a lack of color to a yellow-brown hue indicates the successful dispersion of silver ions within the solution. Upon examination, it was seen that the silver nitrate solution exhibited no change and maintained its original color, which may be attributed to the lack of *M.dubia* leaf extracts. This suggests that the M. dubia extract acts as a reducing agent. A UV spectrometer was used for verification. Subsequently, 24-h samples were examined with a UV spectrometer to measure absorbance in the 200–800 nm range. Previous research has shown that the plasmon surface's absorbance peak (p k) for silver nanoparticles (AgNPs) with a size less than 100 nm is found within the w00–450 nm range. wavelength range [10,11].

Fig. 1 illustrates the changes in the absorbance peak of the synthesized AgNPs. With increased collagen content, the absorbance peaks shifted from 446 nm to 400 nm. The movement was attributed to the reduction in AgNPs, resulting in a correlation between the size of the particles and the absorbance peak in UV–vis spectroscopy. Raza et al. [12] reported the various dimensions of the synthesized AgNPs. The wavelength range used for UV–vis spectroscopy was 397–504 nm. The increase in size of the AgNPs from 10 to 150 nm coincided with this displacement. UV–vis spectroscopy was used to synthesize AgNPs at different lengths. An increase in absorbance peak wavelength from 410 to 490 nm was reported. The occurrence was attributed to the rise in the size of silver particles from 7 nm to 89 nm [13]. The sample without a microwave was shown at a wavelength of 454 nm.

The morphology and shape of the synthesized AgNPs were confirmed using the SEM method. Additionally, the impact of varying doses of the FsCol agent on the structure of the synthesized AgNPs was found to be uniformly spherical. Additional techniques used to produce the AgNPs included green synthesis and microwave-assisted approaches. The scanning electron microscope (SEM) was used to analyze the surface morphology and size of the synthesized AgNPs obtained from both procedures. Upon comparing the synthesized silver nanoparticles generated using two different ways, it was observed that the AgNPs synthesized using the green synthesis method had a rod-like structure and displayed heterogeneity. This result demonstrates the connection between the surface morphology and the scanning electron microscopy (SEM) analysis.

Based on the picture of the scanning electron microscope (SEM), the synthesized silver nanoparticles (AgNPs) produced using the microwave-assisted green synthesis technique exhibited a uniform and spherical shape. Based on the comparison, it was determined that the materials synthesized using the microwave-assisted approach showed a higher rate of synthesis compared to the green synthesis method. Fig. 2 exhibits the scanning electron microscope (SEM) pictures of AgNPs-1 to AgNPs-5.

The EDX spectra of individual particles and aggregates were used for the synthesized AgNPs. The graph demonstrates the presence of elemental silver, as shown by the EDX analysis, which reveals a decrease in the concentration of silver ions and an increase in elemental silver. Conclusive evidence of silver atoms was detected in all samples. The EDX analysis of Ag nanoparticles reveals a natural crystalline structure attributed to reducing silver ions using an extract derived from *M.dubia* leaves.

This investigation has verified the existence of silver nanoparticles derived from *M.dubia*. Furthermore, most of these nanoparticles exhibited distinct energy peaks, indicating the presence of silver atoms at around three keV. According to prior research, the size of silver nanoparticles at an energy level of 3 keV ranged from 5 to 250 nm [14]. Fig. 3 displays the EDX mapping of the synthesized silver nanoparticles, ranging from AgNPs-1 to AgNPs-5.

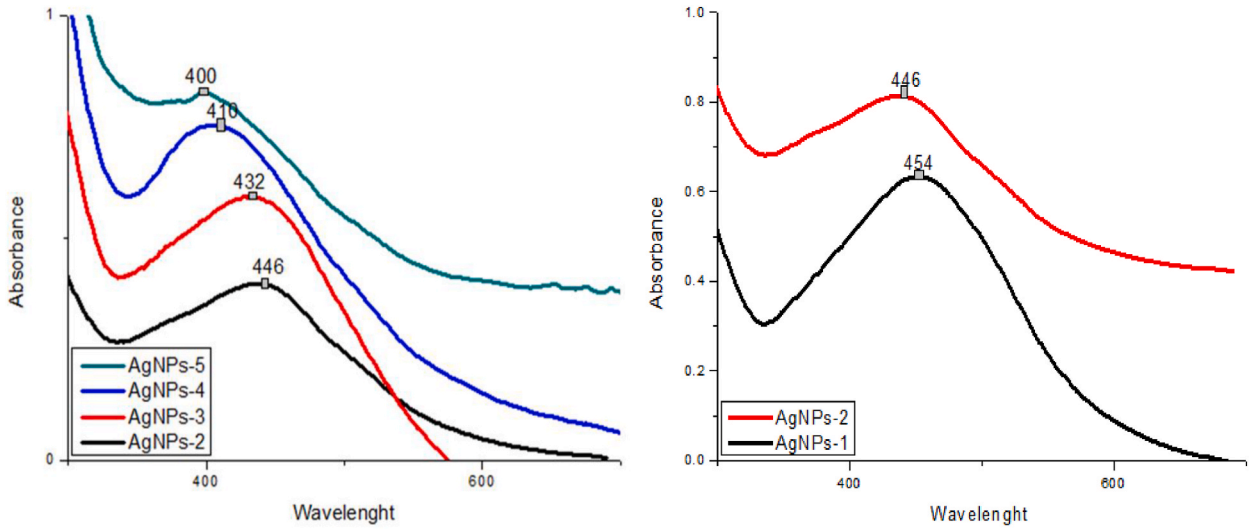

Fig. 1. Uv–vis spectroscopy of synthesized silver nanoparticles (AgNPs-1 to AgNPs-5).

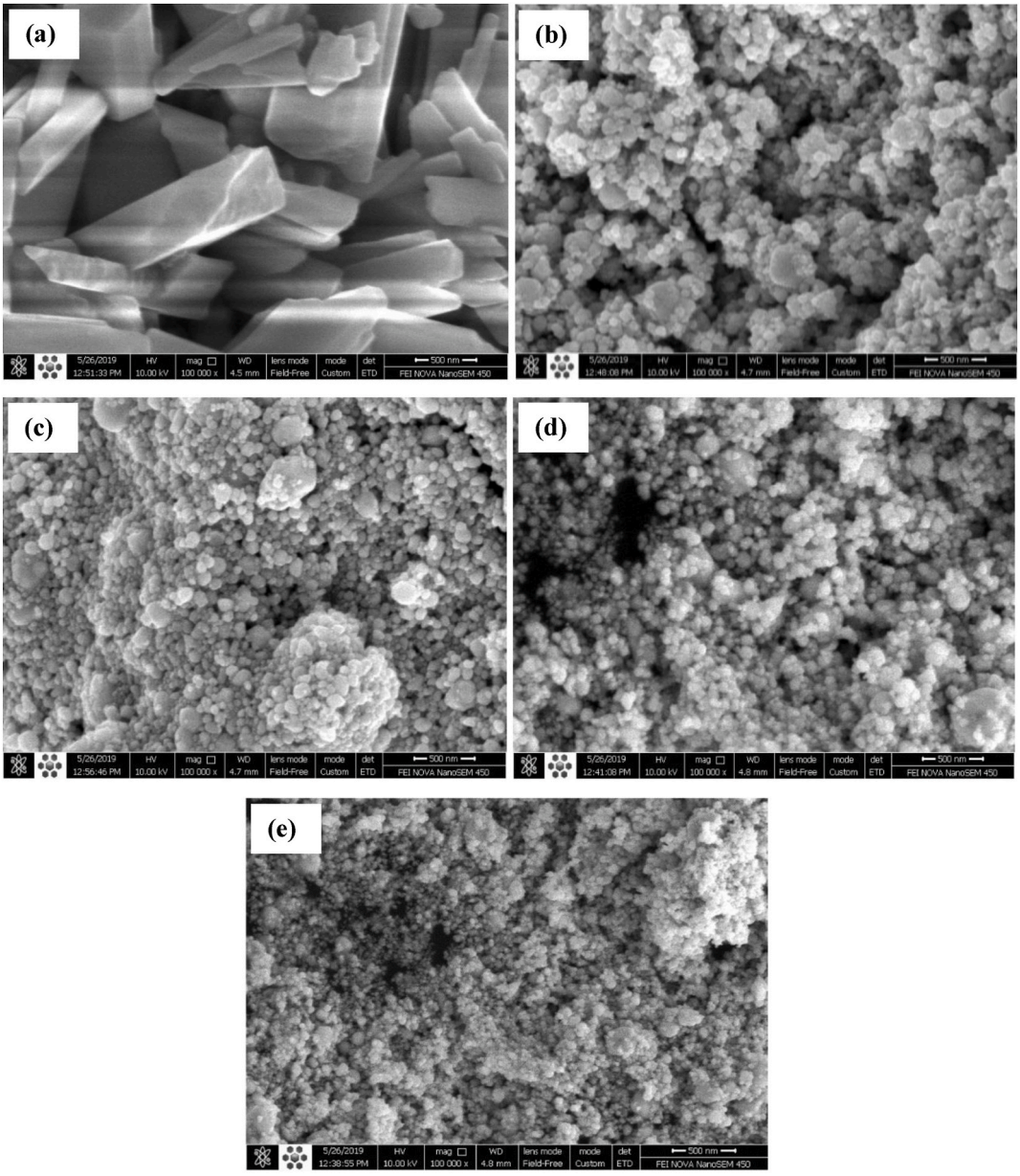

Fig. 2. SEM morphology of a) AgNPs-1, b) AgNPs-2, AgNPs-3, AgNPs-4 and AgNPs-5.

Fig. 3 illustrates the contrast between AgNPs1 and AgNPs2, both synthesized using the microwave-assisted technique with identical component quantities. The figure revealed the detection of silver metallic and the presence of oxygen and carbon. AgNPs1 included a more significant percentage of carbon than silver, while AgNPs2 had a higher rate of silver than carbon. The presence of oxygen and carbon in the plant extract has resulted in the observation of oxygen and carbon peaks, indicating that the AgNPs are surrounded by carbon and oxygen 5]. The EDX spectrum of the three samples revealed the presence of silver in a metallic form—the spectra of silver were seen at 3 KeV in the AgNPs3, AgNPs4, and AgNPs5. Nitrogen, magnesium, carbon, and oxygen were discovered to be present in the sample. The EDX analysis of AgNPs3, AgNPs4, and AgNPs5 revealed that the high silver signal at three keV was primarily due to modest carbon, oxygen, and nitrogen peaks. In addition to the Ag peak, elemental bands corresponding to Mg, N, C, and O may provide information about the origin of a molecule, enzymes, or proteins [16].

The FTIR analysis was performed on the fish collagen, and *M.dubia* leaves to assess the functional groups and compare them with the functional groups of synthesized AgNPs to understand the functional groups surrounding the silver nanoparticles. Fig. 4 displays two prominent peaks in the FsCol spectrum: one at 3441 cm^{-1}, corresponding to the NH (amide A), and another at 1646 cm^{-1}, corresponding to the CO stretching (amide I) [17]. Four small peaks were detected at the following positions: 1548 cm^{-1}, 1466 cm^{-1}, 1392 cm^{-1}, and 1242 cm^{-1}. The peaks at 1548 cm^{-1}-1466 cm^{-1} correspond to the coupling of N–H bends and C–N stretch, specifically

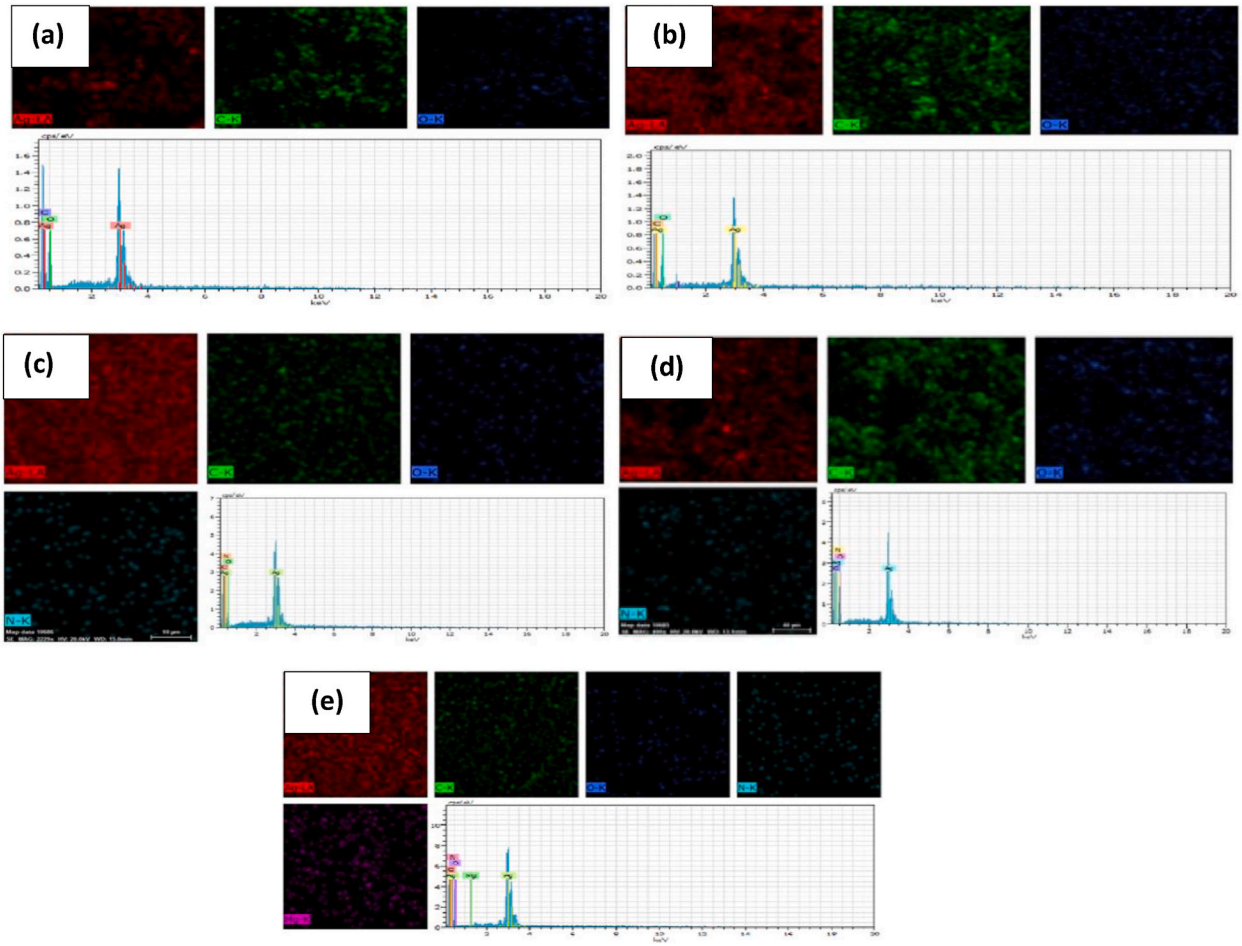

Fig. 3. EDX mapping of a) AgNPs-1, b) AgNPs-2, c) AgNPs-3, d) AgNPs-4 and e)AgNPs-5.

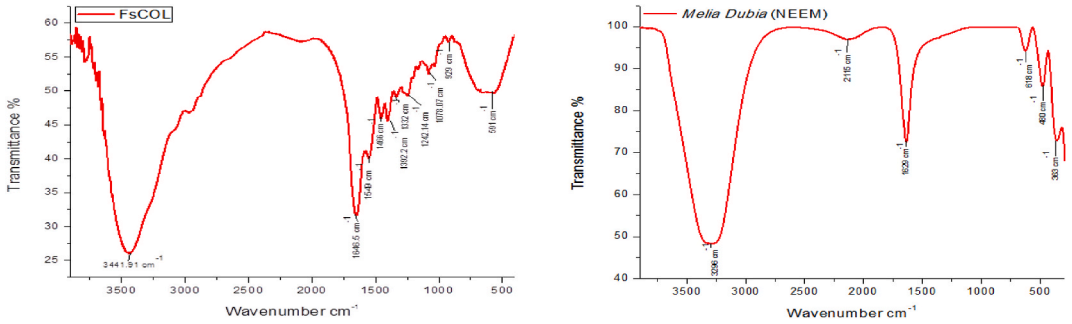

Fig. 4. Ftir of collagen and *M.dubia*.

Amide II. On the other hand, the peaks at 1392 cm^{-1} -1242 cm^{-1} are attributed to N–H bending, also known as Amide III [18].

The leaves of *M.dubia* exhibited two prominent peaks at 3296 cm^{-1} and 1629 cm^{-1}. The peak at 3296 cm^{-1} was attributed to the stretching vibrations of N–H and O–H bonds, which may be attributed to water, alcohol, and phenols (polyphenols) in the M.dubia extract [19]. The band seen at 1629 cm^{-1} was attributed to the amide I functional group. Small peaks were seen at 2115 cm^{-1}, 618 cm^{-1}, 480 cm^{-1}, and 333 cm^{-1}. The band observed at 2115 cm^{-1} in the *M. dubia* extract corresponds to the Alkyne group (C_2H_2) due to phytoconstituents [20]. The bar seen at 618 cm^{-1} was attributed to the presence of C–H bonds in phenolic rings [21], whereas the bar at 480 cm^{-1} indicated the presence of alkyl halides.

A comparison was conducted onto AgNPs-1 with AgNPs-2 as both were synthesized by different methods with the same concentrations. It was discovered that the AgNPs-2 has two major peaks at 3307 cm^{-1} and 1638 cm^{-1}. The peak at 3307 cm^{-1} referred to the

O–H and N–H stretching (amide A), and the peak at 1638 cm^{-1} referred to the stretching of CO, which belongs to amide I. Both of these peaks were observed in AgNPs-1. The peaks at 2140 cm^{-1} referred to the plant components and the peak at 1302 cm^{-1} referred to the N–H bending (Amide III). The peaks at 621 cm^{-1} and 486 cm^{-1} were assigned to the C–H bonds in phenolic rings and alkyl halides, respectively. Fig. 5 displays the FTIR spectrum of the AgNPs-1 and AgNPs-2.

FTIR analysis was conducted onto AgNPs-3, AgNPs-3, and AgNPs-5 to check their factional groups. All samples had shown two major peaks located at 3290 cm^{-1} and 1651 cm^{-1}, which corresponded to the O–H and N–H stretching (amide A) and CO stretching (amide I), respectively. Minor peaks were also observed and have been located at 2140 cm^{-1}, 1226 cm^{-1}, 628 cm^{-1}, and 485 cm^{-1}, which corresponded to the present alkyne group (C_2H_2) because of the phytoconstituents of the *M. dubia* extract, N–H bending (Amide III), to C–H bonds in the phenolic rings and alkyl halides, respectively. Fig. 5 shows the FTIR graph of AgNPs-3, AgNPs-3, and AgNPs-5.

The XRD pattern of AgNPs-1 exhibited distinct peaks at 37.47°, 46.29°, 64.53°, and 77.31°. The diminished intensity of the tiny peaks in the XRD graph may be attributed to bioorganic molecules on the surface of the silver nanoparticles [22]. Fig. 6 depicts a comparison between AgNPs-1 and AgNPs-2, showing peaks at 37.66°, 43.73°, 64.72°, and 77.69°. Several research studies have compared the microwave-assisted green technique with the green synthesis method for synthesizing silver nanoparticles, as described in literature reviews [23]. Nthunya et al. [24] described the production of AgNPs using an alkaline solution of apple extract. The size of the AgNPs obtained by green synthesis was 29 nm, but the AgNPs produced using a microwave-assisted green technique had a size of 22 nm. This suggests that the microwave-assisted green method generates AgNPs of reduced dimensions. The XRD analysis assessed the structure and size of AgNPs-3, AgNPs-4, and AgNPs-5. XRD study of AgNPs-3 revealed diffraction peaks corresponding to silver's face-centered cubic (fcc) structure. The large heights of AgNPs [25] were confirmed by the sharp peaks at 37.49, 42.62, 63.90, and 76.95.

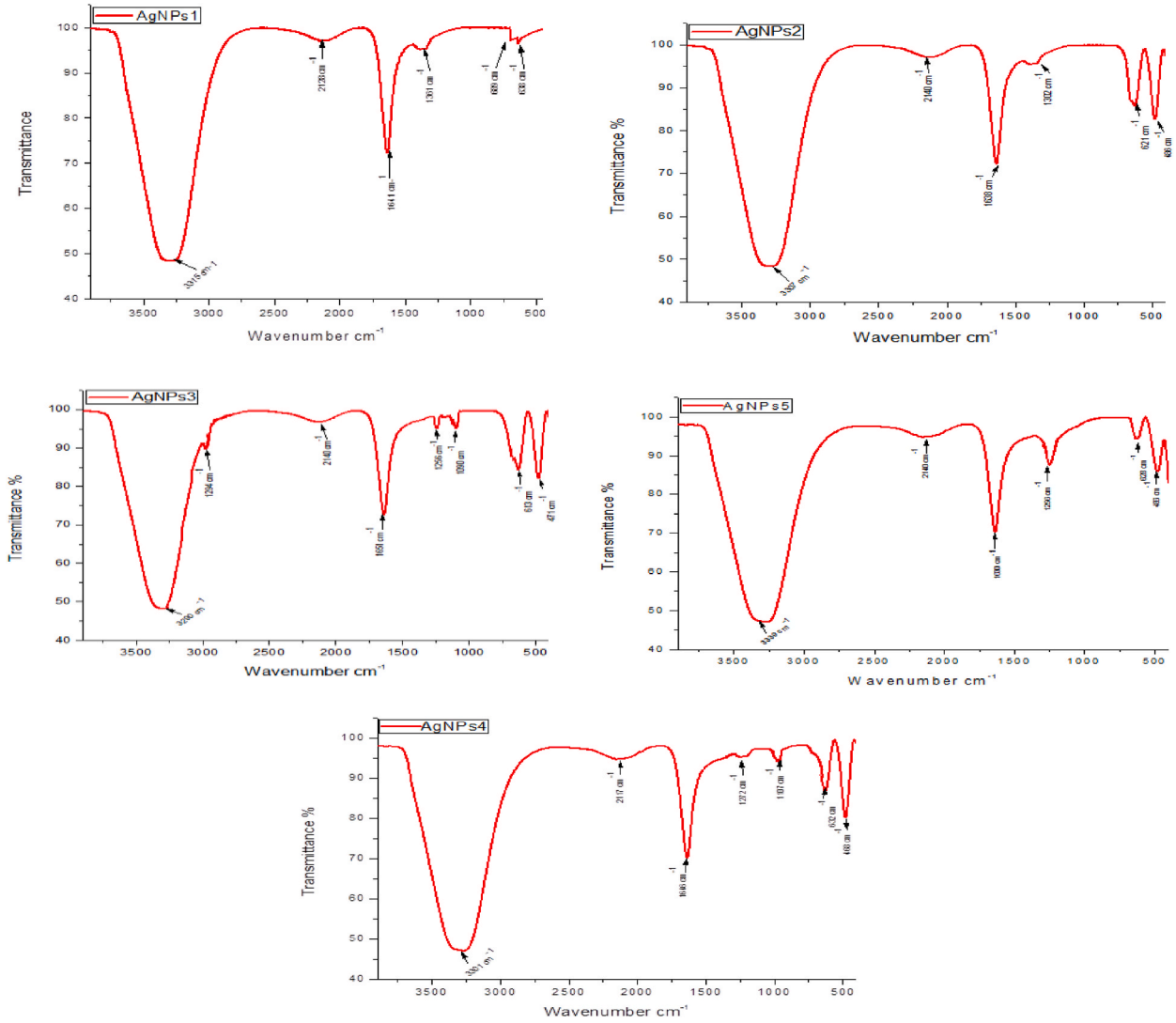

Fig. 5. FTIR spectrum of AgNPs-1, AgNPs-2, AgNPs-3, AgNPs-4 and AgNPs-5.

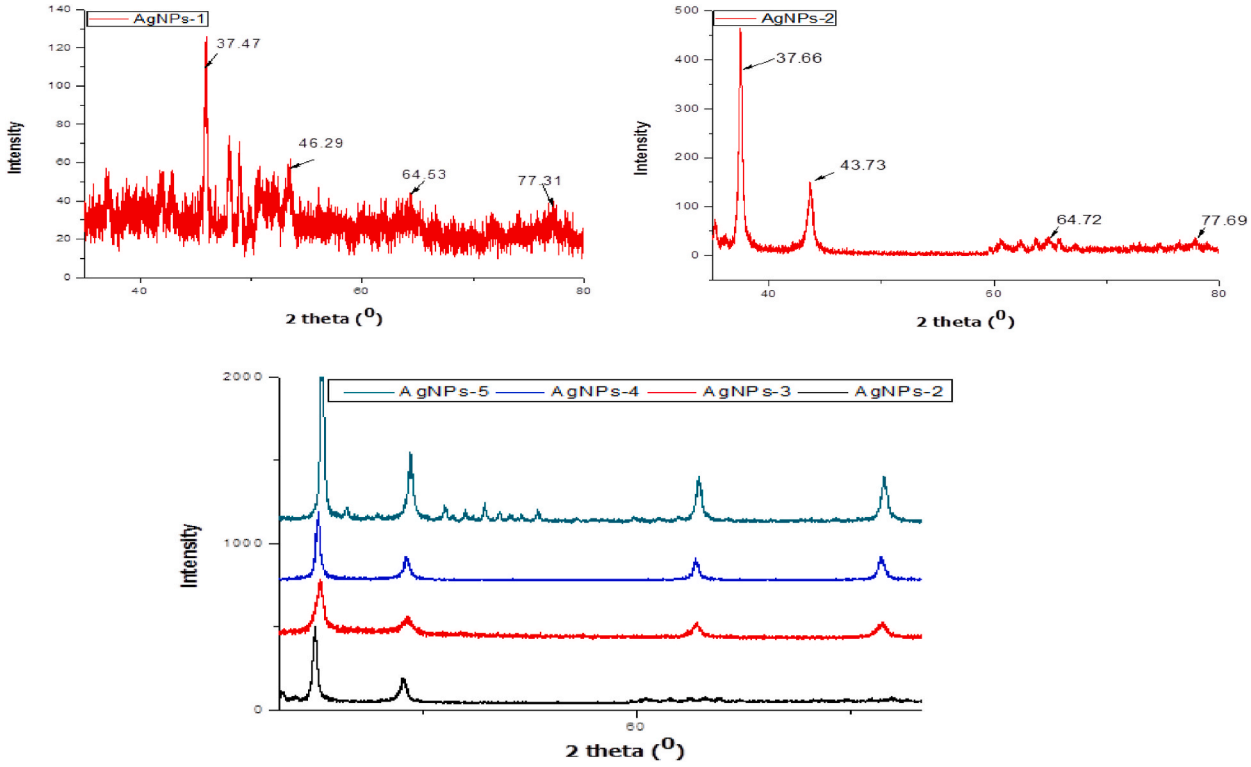

Fig. 6. XRD spectrum of AgNPs-1, AgNPs-2, AgNPs-3, AgNPs-4 and AgNPs-5.

XRD peaks seen in this sample closely matched those reported by Patil et al. [26], who identified peaks at 37.76°, 43.72°, 63.71°, and 76.47°. The XRD pattern indicates that the synthesized AgNPs are crystalline. The XRD analysis was used to identify the crystal structure of AgNPs-4 that were synthesized biologically. The XRD patterns exhibited distinct Bragg's diffraction peaks at angles of 38.72°, 44.08°, 63.78°, and 76.46°. These results aligned with the research findings conducted by Ref. [27]. The production of silver nanoparticles was performed using aqueous extracts derived from Quao Binh Chau and Stereospermum binhchauensis. The X-ray diffraction (XRD) patterns exhibit distinct peaks corresponding to silver nanoparticles at 38.98°, 43.12°, and 63.82°. Research using X-ray diffraction was conducted to gather data on the crystalline characteristics of the synthesized nanoparticles. XRD spectrum of AgNPs-5 showed four distinct peaks with 2θ values of 37.98°, 44.20°, 64.41°, and 77.28°. XRD analysis indicated that the AgNPs-5 exhibits a crystalline structure. The analysis of the XRD patterns for AgNPs-5 revealed that the results closely matched those reported in a previous work conducted by Joseph and Mathew [3]. Their study included the production of AgNPutilizing microwave-assisted green synthesis. In this process, they used the leaf extract of Biophytum sensitivum as a reducing agent. XRD patterns exhibited four distinct peaks with 2θ values of 38.10°, 44.02°, 64.54°, and 77.42°.

The hydrodynamic diameter of both AgNP variations was measured using the DLS (zeta sizer analyzer). The hydrodynamic diameter exhibited the particle size distribution of the AgNP variations and the knowledge of particle dispersion. Based on the comparison of the size of AgNPs-1 and AgNPs-2, AgNPs-1 showed an average size of 437 nm, while AgNPs-2 showed a length of 121 nm. The microwave-assisted resulted in a smaller particle size than the simple green method. Several past works of literature focused on reaching microwave-assisted and simple green techniques. Liem and Nguyen [23] reported the length of synthesized silver nanoparticles using microwave-assisted and simple green synthesis using Mulberry leaves. It was reported that the average size of the silver nanoparticle via simple green synthesis was 20 nm, while the measure through microwave-assisted synthesis was 10 nm. This finding indicated that microwave-assisted green synthesis can form silver nanoparticles rapidly with a smaller size than the simple green synthesis method. A Zeta sizer analyzer was used to examine the impact of fish collagen stabilizer concentrations. The zeta's average of AgNPs-2 was 121 nm, AgNPs-3 was 96.63 nm, AgNPs-4 was 82.62 nm, and AgNPs-5 was 48.50 nm. In general, the AgNPs' size had decreased when the concentration of the FsCol stabilizer had increased. Fig. 7 displays the DLS of AgNPs-1, AgNPs-2, AgNPs-3, AgNPs-4, and AgNPs-5.

The results indicated that the AgNP particles in the microwave-assisted green synthesis were smaller than in green synthesis. The dynamic light scattering (DLS) size is slightly more significant than that of the particle measured using TEM micrographs. Meanwhile, the hydrodynamic radius can be measured through the DLS method [28].

As shown in Fig. 7 the Polydispersity index (PDI) of the samples were ranging from 0.222 to 0.919. The PDI can indicate an increase in the broadness of the dispersed particles' molecular weight or non-spherical shapes. PDI values larger than 0.7 indicate an extensive size distribution of the sample and probably would not be suitable for the DLS technique. PDI values of 0.1–0.2 indicate a

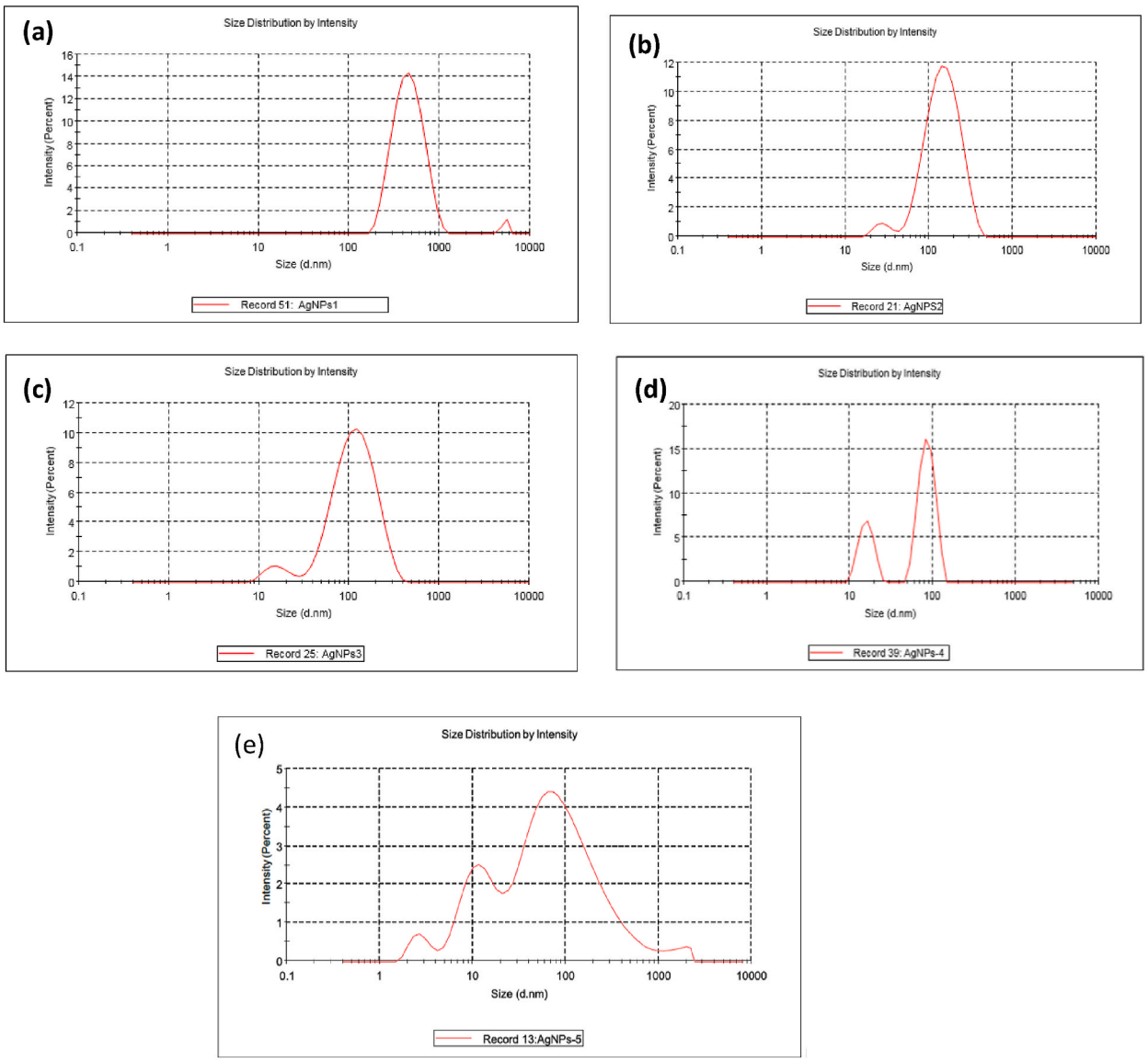

Fig. 7. Dls of (a)AgNPs-1, (b) AgNPs-2, (c) AgNPs-3, (d) AgNPs-4 and (e)AgNPs-5.

monodispersed sample, i.e. almost all particles have the same size and shape. As may be observed from Fig. 7, the average nanoparticle diameter decreased whilst the polydispersity index (PDI) increased upon an increase in temperature. Due to the high PDIs, the z-averages obtained from the DLS do not necessarily represent the actual sizes of the nanoparticles produced [34].

This is due to several limitations this technique poses, including the assumption that all particles dispersed in solution are spherical.

TEM determined the morphology and the size of the particles of AgNPs-2, AgNPs-3, AgNPs-4, and AgNPs-5. A drop of the nanoparticles' suspension was placed on the carbon-coated copper grid to allow the water to evaporate inside a vacuum dryer. This is done to prepare the grid for the TEM analysis of Ag-nanoparticles. Furthermore, the AgNPs-2, AgNPs-3, AgNPs-4, and AgNPs-5 undergo a scanning process using TEM Philips CM-300. The TEM image of the prepared AgNPs-2 is presented in Fig. 8. Based on the image, the nanoparticles of Ag were spherical, with maximum particles in a range of sizes and a mean diameter of 80–100 nm.

Furthermore, they are not in physical contact with one another. Some particles had more than 100 nm due to clumping them together while thawed and putting on the copper grid before the examination. Under STEM (Hitachi SU8020), the image of AgNPs-2 was shown in a spherical shape with particle sizes between 70 and 100 nm in a zeta-sizer analyzer. This is because the particle distribution size was not narrow, and the more significant existing particles may increase light scattering, causing an increment in the particle size values. The measurement of the zeta sizer exhibited larger particles in greater quantity [29]. AgNPs-3 had shown a spherical shape under the TEM analysis with an average size ranging from 60 to 80 nm and 50–80 nm, respectively. Fig. 8 shows the TEM image of AgNPs-3. AgNPs-4 and AgNPs-5 appeared to be spherical under TEM analysis. The average size of AgNPs-4 and AgNPs-5

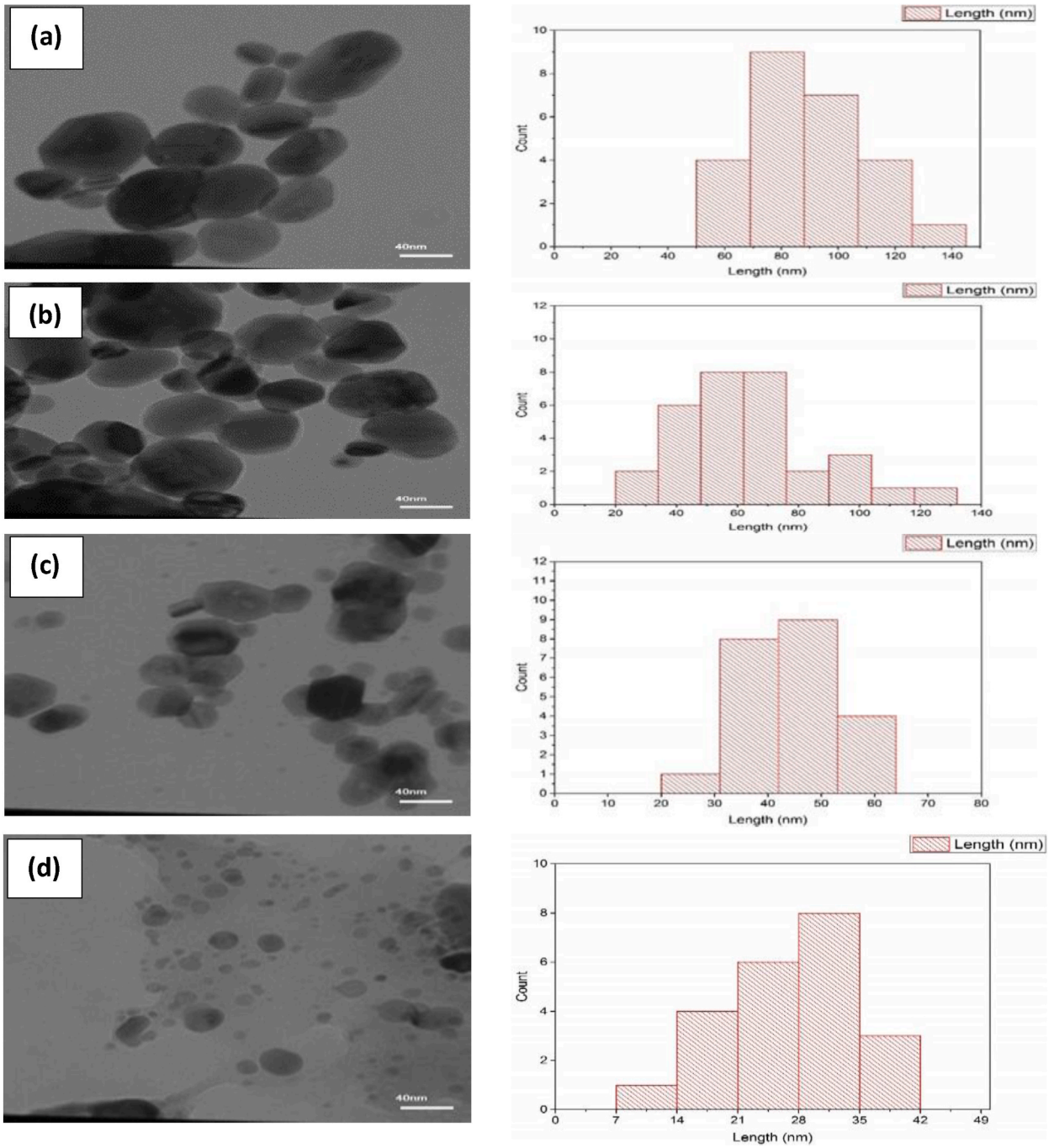

Fig. 8. TEM images of (a) AgNPs-2, (b) AgNPs-3, (c) AgNPs-4 and (d)AgNPs-5.

of TEM, as displayed in Fig. 8, were 40–60 nm and 28–42 nm, respectively. The shape of the AgNPs-2, AgNPs-3, AgNPs-4, and AgNPs-5 appeared to be spherical, corresponding to the SEM results.

The screening process for AgNPs-1, AgNPs-2, AgNPs-3, AgNPs-4, and AgNPs-5 was conducted to identify their antibacterial properties against two bacterial strains. In contrast to the remainder of the S. aureus group, it was discovered that the Staphylococcus aureus is solid and resilient to treatment that uses antibiotics [30].

Fig. 9 presents the variations in the inhibition zones of AgNPs-1, AgNPs-2, AgNPs-3, AgNPs-4, and AgNPs-5. The inhibition zone exhibited the positive and negative control against E. coli. Ampicillin and plant extract were used as the positive control, whereas distilled water and collagen were used as the negative control. Table 1 tabulates the activities of AgNPs-1, AgNPs-2, AgNPs-3, AgNPs-4 and AgNPs-5 against various bacteria. In general, the inhibition zone had increased from AgNPs-1 to AgNPs-5. All samples exhibited

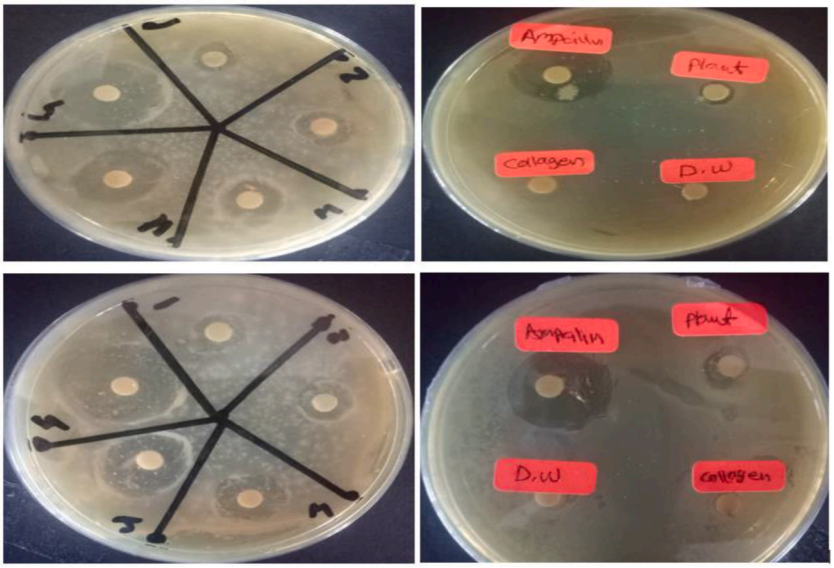

Fig. 9. Anti-bacterial activities of AgNPs-1, AgNPs-2, AgNPs-3, AgNPs-4 and AgNPs-5.

the activities countering to *E. coli and S. aureus.*

The inhibition zone for AgNPs-5 had shown the highest activity against both bacteria, while AgNPs-1 had the lowest training. Previous studies reported that the different sizes of the silver nanoparticles functioned differently against bacteria [15,31]. The size of AgNPs-1 ranged from 150 nm to 400 nm, while the particle size for AgNPs-5 ranged between 28 and 50 nm. This concluded that the impact of silver nanoparticles had increased when the particle size decreased. Kim et al. [32] investigated the biological activity of different lengths of AgNPs against E. coli. As mentioned earlier, the smaller size of AgNPs demonstrated more physical activity than the larger size. Jeong et al. (2014) synthesized and investigated the different sizes of AgNPs for antimicrobial activity. 10 nm and 100 nm had been synthesized and investigated against Methylobacterium spp. The outcome revealed that the 10 nm had exhibited more activities against the bacteria than the 100 nm. Umadevi et al. [33] synthesized the different sizes of AgNPs against Staphylococcus aureus, and Escherichia coli. The finding revealed that the 32 nm particle size had fewer activities than the 20 nm. This concluded that better training can be obtained than in big size. Based on past studies, the increment in the size of Ag nanoparticles causes a reduction in biological efficiency. Therefore, the lower the height of AgNPs, the greater the inhibition of a bacteria zone efficiency.

4. Conclusion

The microwave-assisted green synthesis method was discovered to synthesize the AgNPs successfully. It uses the extract of *M.dubia* as the reducing agent and the FsCol as the stabilizer agent. Four different sizes were obtained by using four different concentrations of FsCol. The smaller AgNPs-5 size was 28–42 nm. The study demonstrated to control of the size of the AgNPs-5 by using 0.6 g of FsCol smaller size based on TEM images. It is concluded that a higher collagen concentration leads to a smaller size for the silver nanoparticles. The bacterial part showed significant ability for all synthesized samples. Moreover, AgNPs-5 showed higher ability; therefore, small sizes of AgNPs exhibit a higher ability to inhibit bacterial growth. The current study demonstrated to obtain a safer, more effective and economy products that can be used as antibiotics in the biomedical filed.

Data availability

The data substantiating the conclusions of this research may be obtained by contacting the corresponding author upon request.

CRediT authorship contribution statement

Mustafa Mudhafar: Writing – review & editing, Writing – original draft, Investigation, Funding acquisition, Formal analysis, Data curation, Conceptualization. **Ismail Zainol:** Formal analysis, Data curation, Conceptualization. **Ameer A.J.:** Methodology, Conceptualization. **Mena Y. Abd:** Funding acquisition. **H.A. Alsailawi:** Methodology, Investigation, Funding acquisition. **Nouby M. Ghazaly:** Data curation. **Rafal Muhammed Hussein:** Project administration. **Mohammed Zorah:** Resources.

Declaration of competing interest

The authors declare the following financial interests/personal relationships which may be considered as potential competing

Table 1
Anti-bacterial activities of AgNPs-1, AgNPs-2, AgNPs-3, AgNPs-4 and AgNPs-5 in mm.

Bacteria	DW	Plant extract	Ampicillin
E. coli	0	8.3	28.2
S. aureus	0	9	26.4

	AgNPs1	AgNPs2	AgNPs3	AgNPs4	AgNPs5
E. coli	11.2	13	14.8	17	22.4
S. aureus	9.8	11.6	13.9	16	20

interests:Ismail Zainol reports financial support and article publishing charges were provided by Sultan Idris University of Education. If there are other authors, they declare that they have no known competing financial interests or personal relationships that could have appeared to influence the work reported in this paper.

Acknowledgements

This research was supported by Ministry of Higher Education, Malaysia through Fundamental Research Grant Scheme 2019-0147-103-02 (FRGS/1/2019/STG07/UPSI/01/1).

References

[1] M.M.K. Peiris, T.D.C.P. Gunasekara, P.M. Jayaweera, S.S.N. Fernando, Bacterial enzyme-mediated synthesis of silver nanoparticles and antimicrobial activity. 4th International Research Symposium on Pure and Applied Sciences, Faculty of Science, University of Kelaniya, Sri Lanka, 2019.
[2] Khalid AbdelRahim, Younis Mahmoud Sabry, Mohamed Ali Ahmed, Khalid Salmeen Almaary, Abd El-Zaher Ma Mustafa, Sherif Moussa Husseiny, Extracellular biosynthesis of silver nanoparticles using Rhizopus stolonifer, Saudi J. Biol. Sci. 24 (1) (2017) 208–216.
[3] Siby Joseph, Beena Mathew, Microwave assisted facile green synthesis of silver and gold nanocatalysts using the leaf extract of Aerva lanata, Spectrochim. Acta Mol. Biomol. Spectrosc. 136 (2015) 1371–1379.
[4] Anal K. Jha, Kamlesh Prasad, Vikash Kumar, K. Prasad, Biosynthesis of silver nanoparticles using Eclipta leaf, Biotechnol. Prog. 25 (5) (2009) 1476–1479.
[5] V. Kathiravan, S. Ravi, S. Ashokkumar, Synthesis of silver nanoparticles from Melia dubia leaf extract and their in vitro anticancer activity, Spectrochim. Acta Mol. Biomol. Spectrosc. 130 (2014) 116–121.
[6] Jolanta Pulit, Marcin Banach, Preparation of nanocrystalline silver using gelatin and glucose as stabilizing and reducing agents,respectively, Dig. J. Nanomater. Biostruct. 8 (2) (2013).
[7] Aleksandra Burkowska-But, Grzegorz Sionkowski, Maciej Walczak, Influence of stabilizers on the antimicrobial properties of silver nanoparticles introduced into natural water, J. Environ. Sci. 26 (3) (2014) 542–549.
[8] Ayman M. Atta, Hamad A. Al-Lohedan, Abdelrahman O. Ezzat, Synthesis of silver nanoparticles by green method stabilized to synthetic human stomach fluid, Molecules 19 (5) (2014) 6737–6753.
[9] Leila Gharibshahi, Saion Elias, Elham Gharibshahi, Abdul Halim Shaari, Khamirul Amin Matori, Influence of Poly (vinylpyrrolidone) concentration on properties of silver nanoparticles manufactured by modified thermal treatment method, PLoS One 12 (2017) 10.
[10] Mustafa Mudhafar, Ismail Zainol, Che Nor Aiza Jaafar, H.A. Alsailawi, Alhussein Arkan Majhool, Microwave-assisted green synthesis of Ag nanoparticles using leaves of Melia dubia (neem) and its antibacterial activities, Journal of Advanced Research in Fluid Mechanics and Thermal Sciences 65 (1) (2020) 121–129.
[11] Arefeh Sadat Dehnavi, Ahmadreza Raisi, Abdolreza Aroujalian, Control size and stability of colloidal silver nanoparticles with antibacterial activity prepared by a green synthesis method, Synth. React. Inorg., Met.-Org., Nano-Met. Chem. 43 (5) (2013) 543–551.
[12] Muhammad Akram Raza, Zakia Kanwal, Anum Rauf, Anjum Nasim Sabri, Saira Riaz, Shahzad Naseem, Size-and shape-dependent antibacterial studies of silver nanoparticles synthesized by wet chemical routes, Nanomaterials 6 (4) (2016) 74.
[13] Martínez Castañon, Gabriel Alejandro, N. Nino-Martinez, F. Martinez-Gutierrez, J.R. Martinez-Mendoza, Facundo Ruiz, Synthesis and antibacterial activity of silver nanoparticles with different sizes, J. Nanoparticle Res. 10 (8) (2008) 1343–1348.
[14] Rajkiran Reddy Banala, Veera Babu Nagati, Pratap Reddy Karnati, Green synthesis and characterization of Carica papaya leaf extract coated silver nanoparticles through X-ray diffraction, electron microscopy and evaluation of bactericidal properties, Saudi J. Biol. Sci. 22 (5) (2015) 637–644.
[15] Sankar Narayan Sinha, Dipak Paul, Nilu Halder, Dipta Sengupta, Samir Kumar Patra, Green synthesis of silver nanoparticles using fresh water green alga Pithophora oedogonia (Mont.) Wittrock and evaluation of their antibacterial activity, Appl. Nanosci. 5 (6) (2015) 703–709.
[16] Anand Barapatre, Keshaw Ram Aadil, Harit Jha, Synergistic antibacterial and antibiofilm activity of silver nanoparticles biosynthesized by lignin-degrading fungus, Bioresources and Bioprocessing 3 (1) (2016) 8.
[17] Ramasamy Sripriya, Ramadhar Kumar, A Novel enzymatic method for preparation and characterization of collagen film from swim bladder of fish rohu (Labeo rohita), Food Nutr. Sci. 6 (15) (2015) 1468.
[18] Phanat Kittiphattanabawon, Sitthipong Nalinanon, Soottawat Benjakul, Hideki Kishimura, Characteristics of pepsin-solubilised collagen from the skin of splendid squid (Loligo formosana), J. Chem. 2015 (2015).
[19] Daizy Philip, Rapid green synthesis of spherical gold nanoparticles using Mangifera indica leaf, Spectrochim. Acta Mol. Biomol. Spectrosc. 77 (4) (2010) 807–810.
[20] Shakeel Ahmed, Mudasir Ahmad Saifullah, Babu Lal Swami, Saiqa Ikram, Green synthesis of silver nanoparticles using Azadirachta indica aqueous leaf extract, Journal of radiation research and applied sciences 9 (1) (2016) 1–7.
[21] Ying Liu, Senghyun Kim, Yeon Ju Kim, Haribalan Perumalsamy, Seungah Lee, Eunson Hwang, Tae-Hoo Yi, Green synthesis of gold nanoparticles using Euphrasia officinalisleaf extract to inhibit lipopolysaccharide-induced inflammation through NF-κB and JAK/STAT pathways in RAW 264.7 macrophages, Int. J. Nanomed. 14 (2019) 2945.
[22] K. Anandalakshmi, J. Venugobal, V. Ramasamy, Characterization of silver nanoparticles by green synthesis method using Pedalium murex leaf extract and their antibacterial activity, Appl. Nanosci. 6 (3) (2016) 399–408.
[23] L. Liem, D. Nguyen, Microwave assisted green synthesis of silver nanoparticles using Mulberry leaves extract and silver nitrate solution, Technologies 7 (1) (2019) 7.
[24] Lebea N. Nthunya, Leonardo Gutierrez, Sebastiaan Derese, Edward N. Nxumalo, Arne R. Verliefde, Bhekie B. Mamba, Sabelo D. Mhlanga, A review of nanoparticle-enhanced membrane distillation membranes: membrane synthesis and applications in water treatment, J. Chem. Technol. Biotechnol. 94 (9) (2019) 2757–2771.
[25] Xihui Zhao, Yanzhi Xia, Qun Li, Xiaomei Ma, Fengyu Quan, Cunzhen Geng, Zhenyu Han, Microwave-assisted synthesis of silver nanoparticles using sodium alginate and their antibacterial activity, Colloids Surf. A Physicochem. Eng. Asp. 444 (2014) 180–188.

[26] Sandeep Patil, Gunjan Chaudhari, Jayasinh Paradeshi, Raghunath Mahajan, Bhushan L. Chaudhari, Instant green synthesis of silver-based herbo-metallic colloidal nanosuspension in Terminalia bellirica fruit aqueous extract for catalytic and antibacterial applications, 3 Biotech 7 (1) (2017) 36.
[27] Ninh Nguyen, Stacy A. Brethauer, John M. Morton, Jaime Ponce, Raul J. Rosenthal (Eds.), The ASMBS Textbook of Bariatric Surgery, Springer International Publishing, 2020.
[28] Tao Huang, Xiao-Hong Nancy Xu, Synthesis and characterization of tunable rainbow colored colloidal silver nanoparticles using single-nanoparticle plasmonic microscopy and spectroscopy, J. Mater. Chem. 20 (44) (2010) 9867–9876.
[29] Taiane GF. Souza, Virgínia ST. Ciminelli, Nelcy Della Santina Mohallem, A comparison of TEM and DLS methods to characterize size distribution of ceramic nanoparticles, J. Phys. Conf. 733 (1) (2016) 012039. IOP Publishing.
[30] Martina Bielaszewska, Alexander Mellmann, Wenlan Zhang, Robin Köck, Angelika Fruth, Andreas Bauwens, Georg Peters, Helge Karch, Characterisation of the Escherichia coli strain associated with an outbreak of haemolytic uraemic syndrome in Germany, 2011: a microbiological study, Lancet Infect. Dis. 11 (9) (2011) 671–676.
[31] El Khoury, ElsyMohamad Abiad, Zeina G. Kassaify, Patra Digambara, Green synthesis of curcumin conjugated nanosilver for the applications in nucleic acid sensing and anti-bacterial activity, Colloids Surf. B Biointerfaces 127 (2015) 274–280.
[32] Sangdoo Kim, Hyunju Kim, Yeong Shin Yim, Soyoung Ha, Atarashi Koji, Guan Tan Tze, Randy S. Longman, et al., Maternal gut bacteria promote neurodevelopmental abnormalities in mouse offspring, Nature 549 (7673) (2017) 528–532.
[33] Yoon Jeong, Dong Woo Lim, Jonghoon Choi, Assessment of size-dependent antimicrobial and cytotoxic properties of silver nanoparticles, Adv. Mater. Sci. Eng. 2014 (2014).
[34] A. Mazzonello, V.V. Valdramidis, C. Farrugia, J.N. Grima, R. Gatt, Synthesis and characterization of silver nanoparticles, Int. J. Morden Eng. Res. 7 (2017) 41–47.